Finite-Element Analysis of Generalized V- and W-Shaped Edge and Broadside-Edge-Coupled Shielded Microstrip Lines on Anisotropic Medium

Yue Yan and Protap Pramanick, *Senior Member, IEEE*

***Abstract*—This paper presents detailed finite-element analysis of generalized V- and W-shaped shielded microstrip lines in an anisotropic medium. The computed results show detailed quasi-static characteristics of the effective dielectric constant, characteristic impedance, and conductor loss of the lines. The broadside edge coupled lines are proposed for the first time in this paper. Unlike the previous analysis based on the conformal mapping method, this analysis takes into account the top walls and sidewalls, finite metallization thickness, and dielectric anisotropy. The results presented in this paper will considerable advance microwave-integrated-circuit technology using V- and W-shaped shielded microstrip lines.**

***Index Terms*—Coupled lines, microstrips, transmission lines.**

I. Introduction

V- AND W-SHAPED shielded microstrip lines recently received considerable attention in microwave-integrated-circuit (MIC) and monolithic-microwave integrated-circuit (MMIC) designs. Fig. 1(a)–(e) shows five possible types of V- and W-shaped microshield lines. The broadside-edge-coupled V-shaped shielded microstrip line and the multicoupled W-shaped shielded microstrip lines are proposed by the authors. These new types of microstrip lines are considered as evolutions form conventional microstrip lines and have reduced radiation loss and electromagnetic coupling. When compared with conventional microstrip or coplanar lines, such lines have the ability to operate without the need for via holes or air bridges for ground equalization. In addition, those offer a wide range of characteristic impedance values. Thus far, a few papers have reported quasi-static analysis of V- and W-shaped shielded microstrip line on isotropic substrate [1]–[4]. These analyses used the conformal mapping method (CMM). Conductor loss in a conventional microstrip was analyzed by Wheeler [5] and Pucel *et al.* [6], [7], where a technique based on the incremental inductance rule was used. The mode-matching method (MMM) and the spectral-domain method (SDM) are applied in the studies [8]–[10]. No doubt the MMM and SDM) are powerful methods for analysis of transmission-line problems, but they do not lead to closed-form analytical equations for the final solution. Besides, their use in the analysis of conductor loss in more general transmission-line problems that involve dielectric medium anisotropy is limited. Keeping in mind the availability of cheaper computing power than ever before, the finite-element method (FEM) and the finite-difference method (FDM) are the two most powerful methods for analysis of shielded microstrip lines of any shape with substrate anisotropy.

This paper presents detailed finite-element analyses of a number of new types of V- and W-shaped shielded microstrip lines with the sidewalls, top shield, finite metallization thickness, and anisotropy of the dielectric substrate. It presents computed results on the various coupling-mode characteristic impedances, effective dielectric constants, and conductor losses.

II. Theory

The characteristic impedances, effective dielectric constants, and conductor loss of microwave transmission lines can be determined from the knowledge of the per-unit-length capacitances of the structures corresponding to the various basic modes. The per-unit-length capacitances of the lines can be obtained by assuming the quasi-TEM mode and using the FEM analysis as follows.

A. Brief Description of the FEM Approach

We first consider a general microshield line with a multiconductor in a finite number of discrete homogeneous iso/anisotropic dielectric regions, as shown in Fig. 2. The conductors can have any arbitrary shape and the enclosure, in general, can have the mixed essential and normal boundary conditions on it. The line is uniform along its longitudinal (z)-axis.

Based on a quasi-TEM model, the potential function Φ in the regions satisfies the two-dimensional Laplace's equation given by

$$\nabla \cdot \left([\varepsilon_r]_j \nabla \Phi_j(x, y) \right) = 0 \tag{1}$$

where $[\varepsilon_r]_j$ is a matrix that represents the dielectric constant

Manuscript received September 22, 1998; revised May 25, 1999. This work was supported by the Natural Sciences and Engineering Research Council of Canada.

Y. Yan is with the Department of Electrical Engineering, University of Saskatchewan, Saskatoon, SK, Canada S7N 5A9.

P. Pramanick is with K&L Microwaves Inc. Salisbury, MD 21801 USA.

Publisher Item Identifier S 0018-9480(01)07592-5.

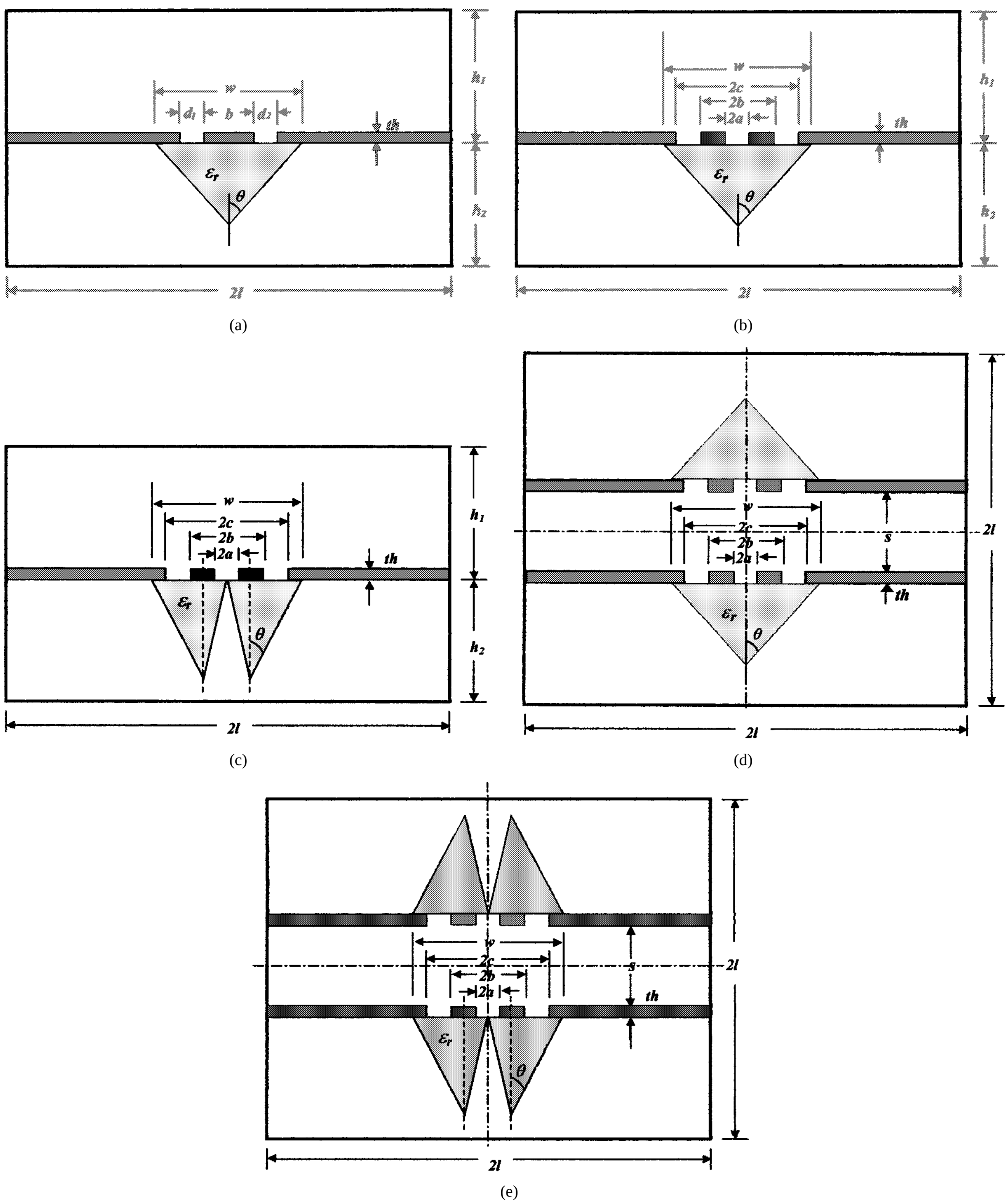

Fig. 1. (a) V-shaped shielded microstrip line. (b) V-shaped coupled shielded microstrip line. (c) W-shaped coupled shielded microstrip line. (d) V-shaped broadside-edge-coupled shielded microstrip line. (e) W-shaped broadside-edge-coupled shielded microstrip line.

tensor of the region j and have different values in x-, y-, or z-directions as follows:

$$[\varepsilon_r]_j = \varepsilon_0 \begin{bmatrix} \varepsilon_{xxj} & \varepsilon_{xyj} & 0 \\ \varepsilon_{xyj} & \varepsilon_{yyj} & 0 \\ 0 & 0 & \varepsilon_{zzj} \end{bmatrix} \tag{2}$$

where

$$\varepsilon_{xxj} = \varepsilon_{\xi j}\cos^2\theta_j + \varepsilon_{\eta j}\sin^2\theta_j \tag{3a}$$

$$\varepsilon_{xyj} = (\varepsilon_{\eta j} - \varepsilon_{\xi j})\sin\theta_j\cos\theta_j \tag{3b}$$

$$\varepsilon_{yyj} = \varepsilon_{\xi j}\sin^2\theta_j + \varepsilon_{\eta j}\cos^2\theta_j \tag{3c}$$

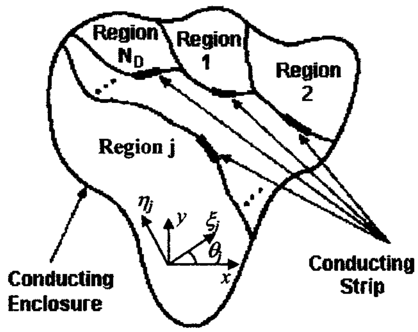

Fig. 2. Generic cross section of microshield line with mixed conductors and dielectrics in conducting enclosure.

as shown in Fig. 2. Expanding (1), we get

$$\varepsilon_{xxj}\frac{\partial^2\Phi_j(x,y)}{\partial x^2}+2\varepsilon_{xyj}\frac{\partial^2\Phi_j(x,y)}{\partial x\partial y}+\varepsilon_{yyj}\frac{\partial^2\Phi_j(x,y)}{\partial y^2}=0. \quad (4)$$

Equation (4) is the basic and most general equation for computing microwave transmission-line characteristics in anisotropic and nonhomogenous structures.

In FEM implementation, the problem region is divided into a large number of cells. We form the finite-element model for (1) by integrating over each mesh cell and applying the divergence theorem to give

$$\int\left([\varepsilon_r]_j\nabla\Phi_j\right)\cdot\bar{n}ds=0 \quad (5)$$

where $\bar{n}$ is the surface unit normal vector, and ds is an element of length along the cell boundary. At the interface between the jth and $(j+1)$th cells, the surface normal terms are assumed to be continuous. Therefore,

$$\left([\varepsilon_r]_j\nabla\Phi_j\right)\cdot\bar{n}=\left([\varepsilon_r]_{j+1}\nabla\Phi_{j+1}\right)\cdot\bar{n}. \quad (6)$$

Since the sense of ds is opposite from the two sides

$$\int_a^b\left[\left([\varepsilon_r]_j\nabla\Phi_j\right)\cdot\bar{n}\right]ds_j=-\int_b^a\left[\left([\varepsilon_r]_{j+1}\nabla\Phi_{j+1}\right)\cdot\bar{n}\right]ds_{j+1} \quad (7)$$

and there is no net contribution to the total integral.

Since the finite-element approximation interpolation reduces to the same function from both adjoining cells, Φ is continuous across a cell interface. This means that the tangential E-field is continuous across the interface, as required by electrostatics. The natural boundary condition specifies the value of $([\varepsilon_r]_j\nabla\Phi_j)\cdot\bar{n}$ at a boundary. Therefore, a surface charge can be represented on internal or external boundary as a nonzero "natural" (or "load") boundary condition. In this case, the interface condition is

$$(D_2-D_1)\cdot\bar{n}=0. \quad (8)$$

This proves that there is no need to "impose" the interface condition of electrostatics at material discontinuities. The condition of continuous $(D\cdot\bar{n})$ and $(E\times\bar{n})$ are automatic. The per-unit-length capacitance can be written as [11]

$$C=\frac{\iint[\varepsilon_r]\left|\nabla\Phi\right|^2dxdy}{(\Phi_2-\Phi_1)^2} \quad (9)$$

where Φ_1 and Φ_2 are the potentials on conductors of interest. The pertinent information regarding the propagation constant and the characteristic impedance is obtained by repeated computations of C for different values of Φ_1, Φ_2, and dielectric constant tensor $[\varepsilon_r]_j$ of different regions.

In our approach to the solution of the problem of the propagation parameters and the conductor losses in the V- and W-shaped single and coupled microshield lines, the unconventional structure and substrate anisotropy are the main issues. The FEM deals with the microshield line by using the appropriate boundary conditions on (1) directly, and finds the scalar potential function Φ satisfying the (1). Thus, the problem of solving the propagation constants and conductor losses in the V- and W-shaped microshield lines is reduced to finding the capacitances of the lines using (9).

B. *Propagation Parameters in Shielded Microstrip Lines*

Once the per-unit-length capacitance C of the transmission line is determined, the characteristic impedance is obtained from [12]

$$Z=\frac{1}{C\cdot v}. \quad (10)$$

The phase velocity v of electromagnetic wave in the line embedded in a dielectric medium is determined from $v=c/\sqrt{\varepsilon_{\text{eff}}}$; here, c is the free-space velocity of the electromagnetic wave and ε_{eff} is the effective dielectric constant of the line. If the dielectric medium is replaced by air, the characteristic impedance of the air-filled line can be obtained from

$$Z^a=\frac{1}{C^a c} \quad (11)$$

where C^a is the capacitance per unit length of the transmission line with dielectrics replaced by air. The effective dielectric constant is computed from

$$\varepsilon_{\text{eff}}=\frac{C}{C^a}. \quad (12)$$

C. *Conductor-Loss Coefficient*

The conductor loss of a microwave transmission line can be characterized by using the attenuation constant α [11]. Calculation of α due to conductor loss is accomplished by using Wheeler's incremental inductance rule and numerical differentiation [13]

An implementation of Wheeler's incremental inductance rule shows that the attenuation constant α_c can be calculated by using the actual structure capacitance C, a new capacitance C' calculated using the dimension of the structure altered by the skin depth δ_s [14], as shown in Fig. 3, and as shown in

$$\alpha_c=\pi\sqrt{\varepsilon_r}\frac{f}{0.2998}\left[1-\left(\frac{C'}{C}\right)\right]\left(\frac{\text{Np}}{\text{m}}\right) \quad (13)$$

where f is the operation frequency in gigahertz and ϵ_r is the dielectric constant of the homogeneous medium. Equation (13), known as Perlow's equation, applies to transmission lines with

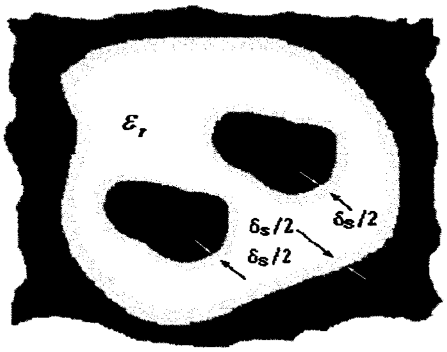

Fig. 3. Reduction of physical dimension by the skin depth δ_s in an arbitrary microshield line.

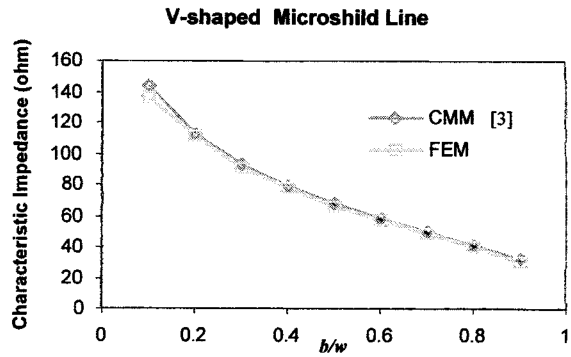

Fig. 4. Characteristic impedances of V-shaped shielded microstrip line calculated using the FEM and CMM, $d_1 = d_2$.

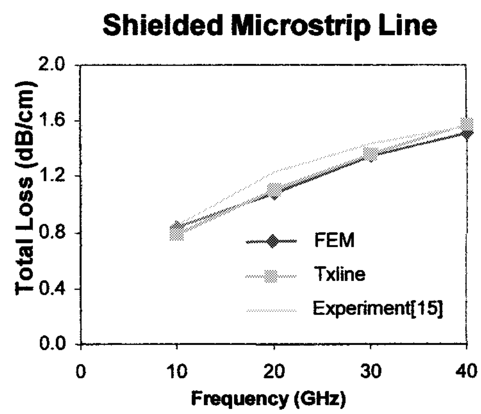

Fig. 5. Total losses of shielded microstrip line. $\varepsilon_r = 12.9$, $\tan\delta = 0.0003$, $h_1 = 2$ mm, $h_2 = 0.1$ mm, $l = 1.2$ mm, $w = 0.01$ mm, $\sigma = 4.1 \times 10^7$ S/m, and $th = 0.003$ mm.

homogeneous dielectric filling only. Therefore, we propose the following generalization of (13):

$$\alpha_c = \pi\sqrt{\varepsilon_{\text{eff}}}\frac{f}{0.2998}\left[1 - \left(\frac{C^{a'}}{C^a}\right)\right]\left(\frac{\text{Np}}{\text{m}}\right) \tag{14}$$

where ε_{eff} is the effective dielectric constant of the nonhomogeneous microwave transmission-line structure, C^a is the capacitance of the air-filled microwave transmission line, and $C^{a'}$ is the capacitance of the air-filled microwave transmission line having the conductor dimension altered by the skin depth, as shown in Fig. 3. Henceforth, we will refer to (14) as the generalized Perlow's equation.

III. Results and Discussions

A. Verification of the Approach and Computer Codes Used

The validity of the proposed approach has been established by comparing the computed results with those obtained by the CMM and a commercial software.[1] In addition, if available, the computed results have been compared with experiment results.

Consider the V-shaped shielded microshield line shown in Fig. 1(a), where $w = 1$ mm, $th = 1/100$ mm, $l = 2$ mm, $h_1 = 3$ mm, $h_2 = w$, $\theta = 30°$, and $\varepsilon_r = 2.55$. This structure cannot be analyzed by the SDM because the substrate is nonplanar. It has been analyzed by the CMM by Kwok and Ian [3]. However, CMM cannot take the finite metallization thickness into consideration. Consequently, loss calculation by combining Wheeler's incremental inductance rule and the CMM is not possible. Fig. 4 shows that the calculations of characteristic impedance of V-shaped shielded microstrip line by our FEM code and the CMM [3] are in excellent agreement. This also validates the generality of the FEM for analysis of newly emerged nonconventional microstrip lines.

To validate our proposed generalization of Perlow's equation (14), we compare the attenuation constants of an open microstrip line computed by our numerical implementation of the generalized Perlow's equation (14) with those computed by the commercial software Txline and published experiment data [15] in Fig. 5. The results agree very closely.

The verification presented in the above sections provides sufficient evidence to support our method of analysis and its generality. We should mention at this point that the proposed generalized equation (14) does not depend on the geometry or the shape of an inhomogeneous two-conductor line. Therefore, since it is valid for an open microstrip line, it should be valid for any other line.

B. Edge-Coupled Lines

If the shielded microstrip line involves two coupled strips, it supports two fundamental TEM modes. The simplest situation is the strips are parallel coupled. Those can be either edge or broadside coupled. The two basic modes are called the even and odd modes. In the even mode, the two strip conductors are excited with equal amplitudes and in-phase (both positive with respect to the ground) potentials and in the odd mode, they are excited with equal amplitudes, but with opposite phases (one positive and the other negative respect to the ground).

We define two characteristic impedances Z_{e} and Z_{o}, where the subscript e and o refer to the even and the odd modes, respectively. The even- and odd-mode impedances can be expressed in terms of the corresponding line capacitances as

$$Z_{\text{e,o}} = \frac{1}{\nu^a\sqrt{C_{\text{e,o}}C_{\text{e,o}}^a}} \tag{15}$$

where C_{e} and C_{o} are the even- and the odd-mode capacitances per-unit-length of edge-coupled lines C_{e}^a and C_{o}^a are the even- and odd-mode capacitances per-unit-length of the edge-coupled

[1]Txline is a transmission-line analysis software based on the MMM. Applied Wave Research, San Diego, CA, 1998.

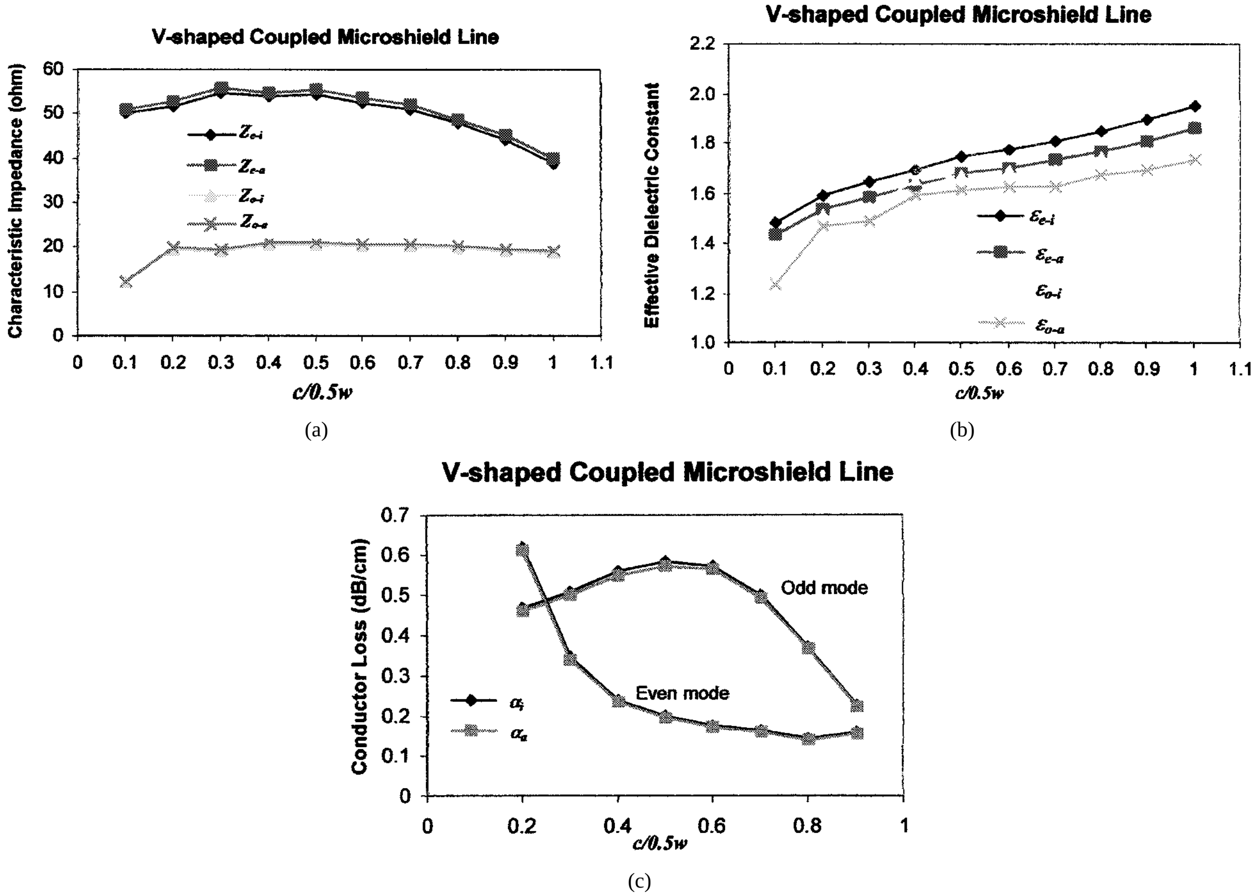

Fig. 6. (a) Characteristic impedances in the V-shaped coupled shielded line with isotropic and anisotropic substrate. (b) Effective dielectric constants in the V-shaped coupled shielded microstrip line with isotropic and anisotropic substrate. (c) Conductor losses in the V-shaped coupled shielded line with isotropic and anisotropic substrate ($f = 20$ GHz).

line when all dielectric materials are replaced by air. Similarly, the effective dielectric constants for the even and the odd modes, represented as $\varepsilon_{\rm effe}$ and $\varepsilon_{\rm effo}$, respectively, can be expressed in terms of the corresponding capacitances as

$$\varepsilon_{\rm effe,o} = \frac{C_{\rm e,o}}{C^{a}_{\rm e,o}}. \tag{16}$$

For the coupled microwave transmission line, the conductor attenuation can be computed by using the following generalized Perlow's equation:

$$\alpha_{\rm e,o} = \pi\sqrt{\varepsilon_{\rm effe,o}}\frac{f}{0.2998}\left[1-\left(\frac{C^{a'}_{\rm e,o}}{C^{a}_{\rm e,o}}\right)\right]\left(\frac{\rm Np}{\rm m}\right) \tag{17}$$

where the original values of capacitance are represented by $C^{a}_{\rm e,o}$ and the new values are calculated using the dimension altered by the skin depth are represented by $C^{a'}_{\rm e,o}$. The effective dielectric constants are represented by $\varepsilon_{\rm effe}$ and $\varepsilon_{\rm effo}$, where the subscripts e and o stand for the even and the odd modes, respectively.

Consider the V-shaped coupled shielded lines shown in Fig. 1(b). $w = 1$ mm, $th = 1/100$ mm, $l = 2$ mm, $h_2 = 1$ mm, $h_1 = 3$ mm, $\theta = 30°$, $a/c = 0.05$, and $b = 0.8(c-a)+a$. The even- and the odd-mode characteristic impedances, the effective dielectric constants and the conductor losses for an isotropic and an anisotropic substrates are shown in Fig. 6(a)–(c), respectively. The subscripts i and a correspond to the isotropic $(\varepsilon_r = 2.55)$ and anisotropic $(\varepsilon_{xx} = 2.44$, $\varepsilon_{yy} = 2.38)$ substrates, respectively.

The computed even-mode characteristic impedances are much larger than the computed odd-mode impedances. Since there is little electric field in the dielectric medium in the even mode, the even-mode characteristic impedance is larger than the odd-mode characteristic impedance. In addition, the odd-mode impedance does not change considerably as the $c/0.5w$ increases. The dielectric anisotropy has very small influence on characteristic impedance. The effective dielectric constant increases as $c/0.5w$ increases because a larger field is concentrated in the substrate. The effect of the dielectric anisotropy is not yet noticeable. The conductor loss is reduced by approximately 0.4 dB/cm when the value of $c/0.5w$ is increased from 0.2 to 0.9 in the even mode. The odd-mode conductor loss has a peak value at $c/0.5w = 0.5$. When the value of $c/0.5w$ is larger or less than 0.5, the conductor loss is reduced. However, the even-mode conductor loss decreases monotonically with $2c/w$.

The W-shaped coupled shielded microstrip line is shown in Fig. 1(c), where $w = 1$ mm, $th = 1/100$ mm, $l = 2$ mm, $h_2 = 1$ mm, $h_1 = 3$ mm, $a/c = 0.05$, and $b = 0.8(c-a)+a$. The W-shaped coupled shielded microstrip line is proposed by the authors. The flare angles of the W-shaped coupled shielded microstrip line depend on the distance between the two strips. The

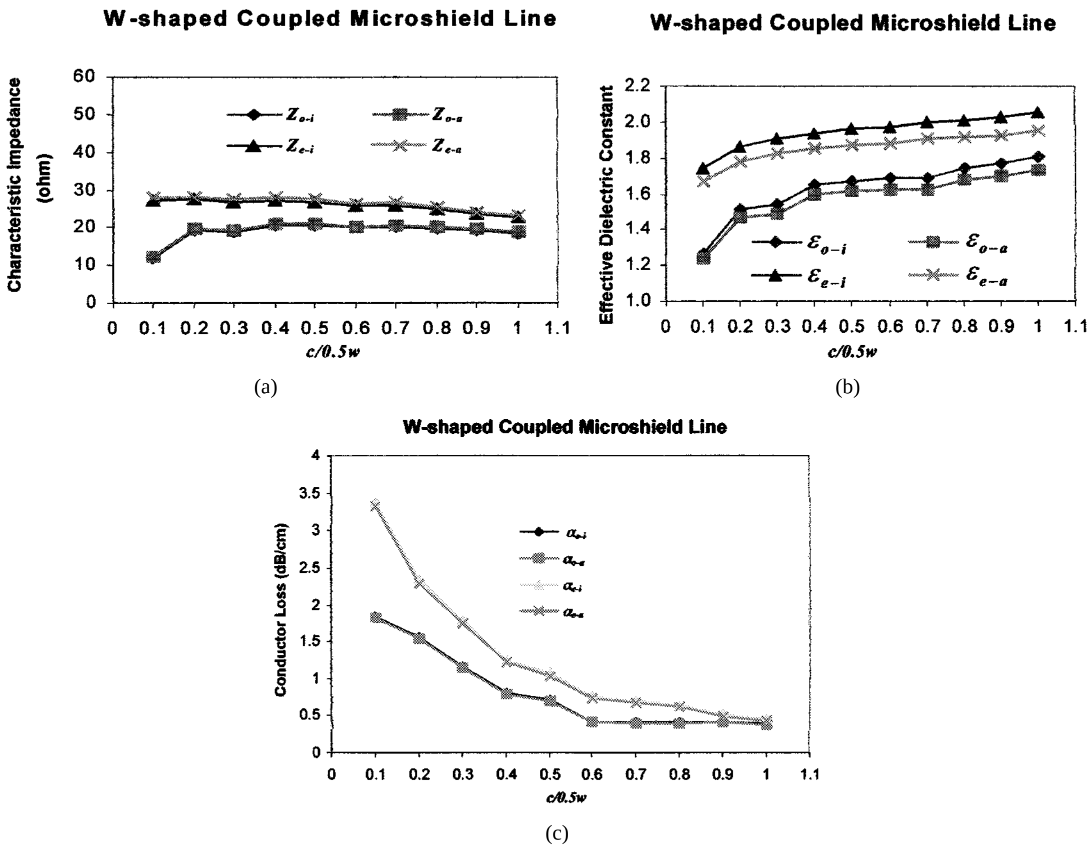

Fig. 7. (a) Characteristic impedance of W-shaped coupled shielded microstrip line with isotropic and anisotropic substrates. (b) Effective dielectric constants of W-shaped coupled shielded microstrip line with isotropic and anisotropic substrates. (c) Conductor losses of W-shaped coupled shielded microstrip line with isotropic and anisotropic substrates.

computed characteristic impedances, effective dielectric constants, and conductor losses of W-shaped coupled shielded lines are shown in Fig. 7(a)–(c), respectively.

Comparing a W-shaped coupled structure with a V-shaped coupled structure (see Figs. 6 and 7), it can be seen that the dielectric shape influences the even-mode characteristic impedances and effective dielectric constants considerably. The even-mode characteristic impedance in W-shaped lines is about 50% of the value in the V-shaped line for comparable geometrical dimension. The even-mode effective dielectric constant in the W-shaped line, on the other hand, is larger than its V-shaped shielded microstrip lines counterpart. In the odd mode, the characteristic impedance almost keeps the same value in both structures. By comparing Fig. 6(b) with Fig. 7(b), one can also notice this behavior in the effective dielectric constant. Comparing Fig. 6(c) with Fig. 7(c), the conductor loss in the V-shaped shielded microstrip line is much less than in the W-shaped microshield line in both the even and the odd modes. Conductor loss in the odd-mode coupled W-shaped line is reduced as $c/0.5w$ increases. However, the conductor loss in V-shaped coupled microshield line has a peak value at $c/0.5w = 0.5$.

C. Broadside-Edge-Coupled Lines

The proposed V- and W-shaped broadside-edge-coupled microshield lines, shown in Fig. 1(d) and (e), combine both edge and broadside coupling. The four strips in this figure have two planes of symmetry, i.e., pp' and qq'. Either an electric wall or a magnetic wall may exist at the symmetry planes depending on the type of excitation. The four modes can be defined [16] as follows:

- even–even mode (ee): pp' magnetic wall, qq' magnetic wall;
- even–odd mode (eo): pp' magnetic wall, qq' electric wall;
- odd–even mode (oe): pp' electric wall, qq' magnetic wall;
- odd–odd mode (oo): pp' electric wall, qq' electric wall.

The characteristic impedances and effective dielectric constants of the four modes, under the quasi-static approximation, are given by

$$Z_{\substack{\mathrm{ee}\\\mathrm{eo}\\\mathrm{oe}\\\mathrm{oo}}} = \frac{1}{c\sqrt{C_{\substack{\mathrm{ee}\\\mathrm{eo}\\\mathrm{oe}\\\mathrm{oo}}} C^{a}_{\substack{\mathrm{ee}\\\mathrm{eo}\\\mathrm{oe}\\\mathrm{oo}}}}} \tag{18}$$

$$\varepsilon_{\substack{\mathrm{effee}\\\mathrm{effeo}\\\mathrm{effoe}\\\mathrm{effoo}}} = \frac{C_{\substack{\mathrm{ee}\\\mathrm{eo}\\\mathrm{oe}\\\mathrm{oo}}}}{C^{a}_{\substack{\mathrm{ee}\\\mathrm{eo}\\\mathrm{oe}\\\mathrm{oo}}}} \tag{19}$$

where C_{ee}, C_{eo}, C_{oe}, and C_{oo} are the line capacitances per unit length of the structure for the four propagation modes, C^a_{ee}, C^a_{eo}, C^a_{oe}, and C^a_{oo} are the corresponding capacitances of the structure when all dielectrics are replaced by air, and c is the velocity of electromagnetic wave in free space.

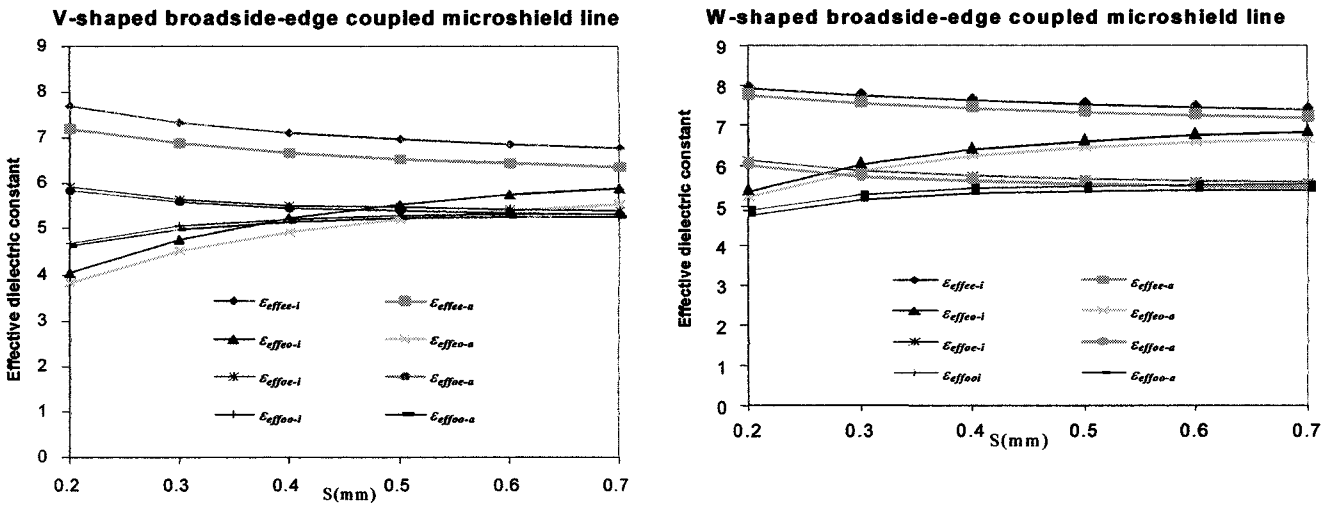

(a) (b)

Fig. 8. (a) Effective dielectric constant as functions of air gap in V-shaped broadside-edge-coupled microshield line (see Fig. 1(d) for the geometrical parameters). (b) Effective dielectric constants as functions of air gap in W-shaped broadside-edge-coupled microshield line (see Fig. 1(e) for the geometrical parameters).

For the broadside-edge-coupled microshield lines, (14) can be written as

$$\alpha_{\substack{ee\\eo\\oe\\oo}} = \pi\sqrt{\varepsilon_{\substack{\mathrm{effee}\\\mathrm{effeo}\\\mathrm{effoe}\\\mathrm{effoo}}}}\,\frac{f}{0.2998}\left[1-\left(\frac{C^{a'}_{\substack{ee\\eo\\oe\\oo}}}{C^{a}_{\substack{ee\\eo\\oe\\oo}}}\right)\right]\left(\frac{\mathrm{Np}}{\mathrm{m}}\right). \quad (20)$$

The original values of capacitances are

$$C^{a}_{\substack{ee\\eo\\oe\\oo}}$$

the new values, calculated using the dimension altered by the skin depth, are given by

$$C^{a'}_{\substack{ee\\eo\\oe\\oo}}$$

and the effective dielectric constants are

$$\varepsilon_{\substack{\mathrm{effee}\\\mathrm{effeo}\\\mathrm{effoe}\\\mathrm{effoo}}}$$

respectively.

The following calculations and discussions on V- and W-shaped broadside-edge-coupled microshield lines are based on the FEM method described and discussed above. The substrates are considered to be both isotropic $(\varepsilon_r = 10)$ and anisotropic $(\varepsilon_{xx} = 9.4, \varepsilon_{yy} = 11.6)$. The sidewalls of the microshield line and the thickness of the strip conductors have also been taken into consideration. The computed even–even, even–odd, odd–even, and odd–odd mode effective dielectric constants of the V- and W-shaped broadside-edge-coupled microshield lines, in both isotropic and anisotropic substrates, are presented in Fig. 8(a) and (b). Subscripts i and a correspond to isotropic and anisotropic dielectric substrates, respectively. The effective dielectric constants are presented as functions of the conductor strip separation s in the vertical direction, as shown in Fig. 1(d) and (e).

For a V-shaped broadside-edge-coupled microshield line, the separation air gap s between the two substrates affect the effective dielectric constants in different ways, depending on the mode of the broadside coupling. As s increases, the effective dielectric constant of the broadside even-mode coupling (even–even and odd–even modes) decreases, but the effective dielectric constant of broadside odd-mode coupling (the even–odd and odd–odd modes) increases. This behavior of effective dielectric constant can also be seen in the W-shaped structure [see Fig. 8(b)], but the increase and decrease are reduced.

The computed characteristic impedances of the V- and W-shaped broadside-edge-coupled microshield lines are plotted in Fig. 9(a) and (b) respectively. For the V-shaped structure [see Fig. 9(a)], the characteristic impedances of the even–odd mode greatly depend on the separation s. The amount of variation in characteristic impedance is about 30% over the $0.2 < s < 0.7$ (mm) range. For the other modes, the amount of variation is less than 10% in the same range of s. The characteristic impedances are affected by the edge coupling considerably. For edge even-mode couplings (even–even and even–odd modes), the characteristic impedances are twice those of the edge odd-mode couplings (odd–even and odd–odd modes) in V-shaped broadside-edge-coupled microshield lines. The W-shape substrate greatly reduces the characteristic impedance in W-shaped broadside-edge-coupled microshield line. For a comparable set of geometrical dimensions, the W-shaped broadside-edge-coupled microshield line has only one-half the characteristic impedance of the V-shaped broadside-edge-coupled microshield line in the edge even-mode coupling.

Fig. 10(a) and (b) shows the conductor losses in the V- and W-shaped broadside-edge-coupled microshield lines. The operation frequency $f = 1.5$ GHz. It is observed that the average conductor losses in the V-shaped broadside-edge-coupled microshield line are less than those in the W-shaped broadside-edge-coupled line. For the V-shaped structure, the conductor losses in the edge even-mode coupling are less than those

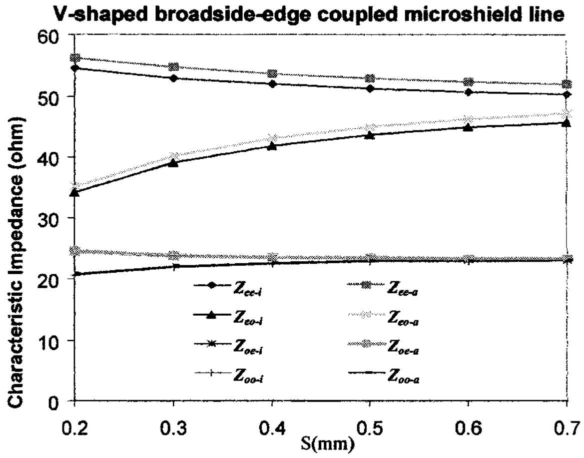

(a)

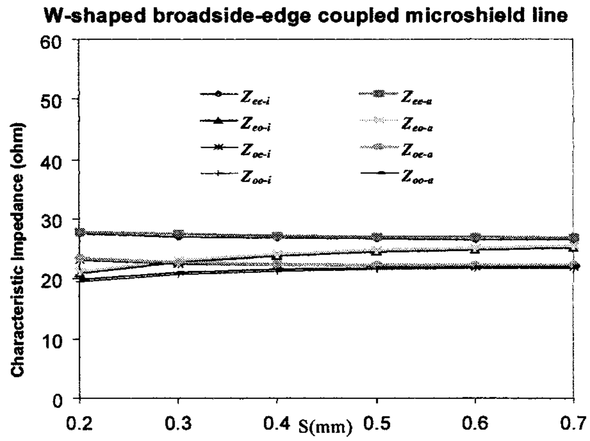

(b)

Fig. 9. (a) Characteristic impedance of V-shaped broadside-edge-coupled microshield lines isotropic and anisotropic substrates. (b) Characteristic impedance of W-shaped broadside-edge-coupled microshield line on isotropic and anisotropic substrates.

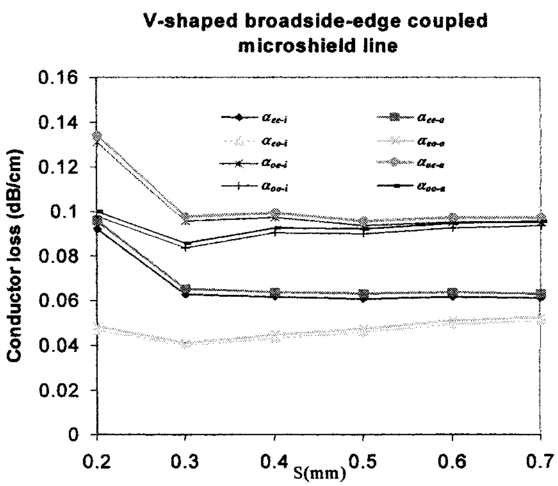

(a)

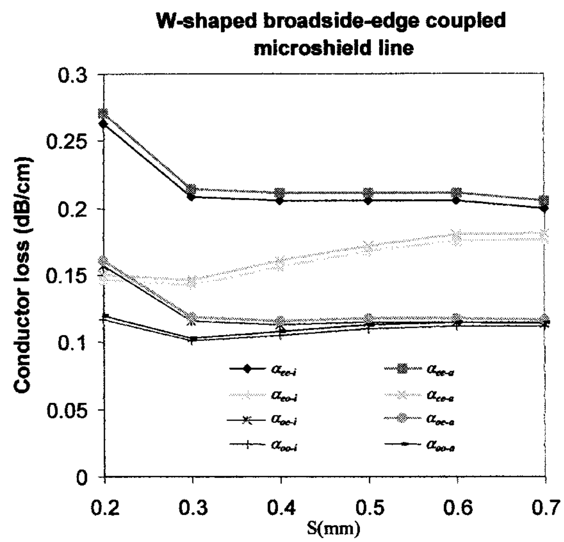

(b)

Fig. 10. (a) Conductor losses for the variations of mode and substrate for V-shaped broadside-edge-coupled shielded microstrip line ($f = 1.5$ GHz). (b) The even- and the odd-mode conductor losses of W-shaped broadside-edge-coupled shielded microstrip lines on isotropic and anisotropic substrates ($f = 1.5$ GHz).

in the edge odd-mode coupling. However, for the W-shaped structure, the conductor losses in the edge even-mode coupling are larger than those in the edge odd-mode coupling. The thickness of air layer s dose not influence the conductor loss considerably when $s > 0.3$ mm in both V- and W-shaped structures for the structural parameters shown in Fig. 1(d) and (e).

IV. Conclusion

V- and W-shaped single and coupled microshield lines have been studied in this paper. The characteristic impedances, effective dielectric constants, and conductor losses have been calculated using the FEM. The results are compared with those obtained by the CMM. The analysis considers the effects of the sidewalls, top shield, and the substrate anisotropy. The results of the analyses show that the shape of the structures considerably affect the even-mode characteristic impedance, the effective dielectric constant, and the conductor loss, but the effects are very small on the odd-mode parameters in case of coupled lines. We have also noted that substrate anisotropy has very little effect on the conductor loss. Our analyses have shown that the V- and W-shaped microshield lines offer flexibility in microwave-circuit designs. The shield substrate and shapes can be used to adjust the propagation parameters and the conductor losses as extra parameters. These analysis results can be used in the design of MICs and MMICs.

References

[1] N. Yuan, C. Ruan, and W. Lin, "Analytical analyses of V, elliptic, and circular-shaped microshield transmission lines," *IEEE Trans. Microwave Theory Tech.*, vol. 42, pp. 855–858, May 1994.

[2] N. Yuan, C. Ruan, W. Lin, J. He, and C. He, "Coplanar coupled lines: The effect of the presence of the lateral ground planes, upper and lower ground planes, and the V-shaped microshield ground walls," *Proc. Inst. Elect. Eng.*, pt. H, vol. 142, no. 1, pp. 63–65, Feb. 1995.

[3] K. M. Cheng and I. D. Robertson, "Simple and explicit formulas for the design and analysis of asymmetrical V-shaped microshield line," *IEEE Trans. Microwave Theory Tech.*, vol. 43, pp. 2501–2504, Oct. 1995.

[4] ——, "Quasi-TEM study of microshield lines with practical cavity sidewall profiles," *IEEE Trans. Microwave Theory Tech.*, vol. 43, pp. 2689–2694, Dec. 1995.

[5] H. A. Wheeler, "Formulas for the skin effect," in *Proc. IRE.*, vol. 30, 1942, pp. 412–424.

[6] R. A. Pucel *et al.*, "Losses in microstrip," *IEEE Trans. Microwave Theory Tech.*, vol. MTT-16, pp. 342–350, June 1968.

[7] ——, "Corrections to 'Losses in microstrip'," *IEEE Trans. Microwave Theory Tech.*, vol. MTT-16, p. 1064, Dec. 1968.

[8] W. Heinrich, "Full-wave analysis of conductor losses on the MMIC transmission lines," in *IEEE MTT-S Int. Microwave Symp. Dig.*, 1989, pp. 911–914.

[9] R. N. Simons *et al.*, "Channelized coplanar waveguide: Discontinuities, junctions, and propagation characteristics," in *IEEE MTT-S Int. Microwave Symp. Dig.*, 1989, pp. 915–918.

[10] T. E. van Deventer, P. B. Katehi, and A. C. Changellaris, "High frequency conductor and dielectric losses in shielded microstrip," in *IEEE MTT-S Int. Microwave Symp. Dig.*, 1989, pp. 919–922.

[11] R. E. Collin, *Field Theory of Guided Waves*. New York: IEEE Press, 1992.

[12] Z. Pantic and R. Mittra, "Quasi-TEM analysis of microwave transmission lines by the finite-element method," *IEEE Trans. Microwave Trans. Microwave Theory Tech.*, vol. MTT-34, pp. 1096–1103, Nov. 1986.

[13] H. A. Wheeler, "Transmission-line properties of a strip on a dielectric sheet on a plane," *IEEE Trans. Microwave Theory Tech.*, vol. MTT-25, pp. 631–641, Aug. 1977.

[14] S. M. Perlow, "Analysis of edge coupled shielded strip and slabline structures," *IEEE Trans. Microwave Theory Tech.*, vol. MTT-35, pp. 522–529, May 1987.

[15] M. E. Goldfarb and A. Platzker, "Losses in GaAs microstrip," *IEEE Trans. Microwave Theory Tech.*, vol. 38, pp. 1957–1963, Dec. 1990.

[16] B. Bhat and S. K. Koul, *Stripline-Like Transmission Lines or Microwave Integrated Circuits*. New York: Wiley, 1989.

Yue Yan, photograph and biography not available at time of publication.

Protap Pramanick (S'83–M'84–SM'88) received the B.Tech degree (with honors) in electronics and telecommunication engineering from the Indian Institute of Technology, Kharagpur, India, in 1977, and the Ph.D. degree in microwave engineering from the Indian Institute of Technology, Kanpur, India, in 1982.

In 1982, he joined the Department of Electrical Engineering, University of Ottawa, Ottawa, ON, Canada, as a Post-Doctoral Fellow. In 1984, he joined the Canadian Marconi Corporation, Ottawa, ON, Canada, as a Senior Design Specialist in the Avionics Division. In April 1986, he joined Com Dev Ltd., Cambridge, ON, Canada. From July 1992 to April 2000, he was an Associate Professor in the Department of Electrical Engineering, University of Saskatchewan, Saskatoon, SK, Canada. He is currently with K&L Microwave Inc., Salisbury, MD. He is also an Adjunct Professor at the Hansen School of Science and Technology, Salisbury University, Salisbury, MD. He is also the Chief Executive Officer (CEO) of Polar Waves Consulting (PWC). PWC currently provides services to Motorola and Ericsson, as well as many other companies. He has authored or co-authored many publications in the area of microwave integrated circuits. He co-edited *E-plane Integrated Circuits* (Norwood, MA: Artech House, 1987), and has contributed to *Topics in Millimeter Wave Technology* (New York: Academic, 1988), *Microwave Solid State Circuit Design* (New York: Wiley, 1988), and the *Handbook of Microwave Engineering* (New York: Academic, 1995). He holds several patents in filters for cellular radio. He is on the Editorial Review Board of the *International Journal of Microwave and Millimeter-Wave Computer-Aided Engineering*.

Dr. Pramanick is on the Editorial Review Board of the IEEE TRANSACTIONS ON MICROWAVE THEORY AND TECHNIQUES.